



Accuracy of Computer-Aided Evaluation of the Relationship between Mandibular Third Molar and Mandibular Canal on CBCT Images using Deep Learning Model (Artificial Intelligence): Diagnostic Accuracy Study.

Ahmed Magdy¹, Enas Anter², Ali Khater Mohamed³, Mushira M. Dahaba⁴, Yara Helaly⁵

¹Ahmed Magdy, BDs, MSc, Oral and Maxillofacial Radiology Department, Cairo university, Cairo, 12613, Egypt.

²Enas Anter, BDs, Msc, PhD Oral and Maxillofacial Radiology Department, Cairo university, Cairo, 12613, Egypt.

³ Ali Khater Mohamed, Department of Computer Science, Faculty of Computer Science, October University for Modern Sciences and Arts (MSA), 6th October City, Giza 12451, Egypt

⁴Mushira M.Dahaba, Oral and Maxillofacial Radiology Department, Cairo university, Cairo, 12613, Egypt.

⁵Yara Helaly, BDs, Msc, PhD Oral and Maxillofacial Radiology Department, Cairo university, Cairo, 12613, Egypt.

(Received: 16 September 2024

Revised: 11 October 2024

Accepted: 11 December 2024)

KEYWORDS

artificial intelligence;
CNN ; deep learning;
Mandibular canal ;
Inferior alveolar
canal; impacted 3rd
molar ; cone beam
computed
tomography; CBCT.

ABSTRACT:

Aim: The purpose of this study was to assess the accuracy of a newly developed deep learning model in automatic evaluation of the relationship between mandibular third molar (M3M) and the mandibular canal (MC) on cone beam computed tomography (CBCT) images by comparing it with experienced radiologist opinion.

Methodology: CBCT scans of 184 patients were imported to 3d slicer software. The Radiologist-dependent MC - M3M relation was performed on the axial cuts and then classified into 3 classes: cancellous bone separation, contact with intact cortex and contact with interrupted cortex by 2 Oral and Maxillofacial Radiologists (OMFR) and this classification serves as the ground truth. The annotated data was divided into two groups: 80% for training and validation and 20 % for testing. The data was used to develop the AI model in based on CNN. Confusion matrix and receiver-operating characteristic (ROC) analysis were used in the statistical evaluation of the results of the classification model.

Results: The Average accuracy, precision, recall and F1 score for testing was 0.79, 0.77, 0.77 and 0.77 respectively, while for training was 0.9, 0.91, 0.9 and 0.9 respectively.

Conclusion: Our deep learning model based on CNN showed outstanding performance in the evaluation of the relation between MC and M3M on CBCT images. However, further development is needed with high quality data to improve the algorithm and validate the accuracy using external validation data sets.

Introduction:

The impacted mandibular third molar (M3M) extraction, considered one of the most common surgeries in oral and maxillofacial field, it can be associated with several postoperative complications, like pain, bleeding, swelling, and inferior alveolar nerve (IAN) injury or complete damage, impairing the quality of life of the affected

patients. The incidence of temporary IAN injury caused by M3M extraction was 0.4–8.4%, while the incidence of permanent injury is less than 1%[1]. However, due to the high occurrence of impacted M3M, a large number of patients suffer from IAN injury caused by impacted M3M extraction[2].



The most significant risk factor of IAN injury caused by M3M extraction is the proximity of the root of the M3M to the mandibular canal(MC)[3]. So, comprehensive preoperative analysis and evaluation of the anatomical structures are essential before impacted M3M extraction to decrease the IAN injury risk. The panoramic radiography is not that much accurate in displaying the relation between impacted M3M extraction and IAN due to the superimposition and inherent limitations.

The accuracy of predicting the probability the IAN injury during the impacted M3M extraction using panoramic radiographs were controversial[4]. Cone beam computed tomography (CBCT), A (3D) imaging modality, provides accurate 3D information with decreased radiation dose than medical CT [5]. It was demonstrated that CBCT was a better and accurate radiographic method than panoramic radiography for evaluating the relationship between impacted M3M and (IAN) [6]. So that, CBCT has been considered as the modality of choice for preoperative assessment of complicated M3M extraction [7].

Deep learning, one of artificial intelligence subsets, had a rapid progression and has a significant role in medical fields. One of the deep learning models, guided learning of the convolutional neural network (CNN) is recently investigated, which has been proven to surpass human judgmental level in many medical imaging fields[8, 9]. After CNN was introduced to the maxillofacial field, it was used for the assessment ,detection, categorization, and segmentation of the surrounding anatomical structures

[10]. Recently, deep learning based on CNN models has been used for the impacted M3M and MC detection and segmentation on panoramic radiographs and CBCT [11], the classification and staging of development, and the approximation measurements of the impacted M3M on panoramic radiographs.

Fukuda et al. compared 3 CNNs for classification of the impacted M3M and MC relation with panoramic radiographs [12]. Yoo et al. proposed a CNN-based approach to assess the stalemate of the impacted M3M extraction using panoramic radiographs [13]. So, as mentioned before, panoramic

radiography can't accurately describe the anatomical structures due to the superimposition that happens

in the (2D) imaging modalities. Orhan et al. reported an AI application (Diagnocat, Inc.) based on CNN with high precision in detecting the M3M and assessment of the number of roots related to adjacent anatomical structures [14].

Methodology:

Study design

This is a retrospective type of study, where the data collection was considered before the performance of index tests and reference standard. The results are presented in terms of accuracy, sensitivity (Recall), positive predictive value (Precision), and receiver operating characteristic curve, thus categorizing it as a diagnostic accuracy study.

This study was conducted under the consent of the Research Ethics Committee of the Faculty of Dentistry, Cairo University, on January 5, 2022, and adheres to the Declaration of Helsinki (2013).

Sample Size Calculation

A power analysis was designed to have adequate power to apply a two-sided statistical test of the null hypothesis that results of deep learning model are as accurate as the radiologist

opinion. By adopting a (95%) confidence interval and by using a specificity value of (88.0%) of the DL group based on the results of a previous study [15] and 100 % for the ground truth: sample size calculated based on specificity was 50 samples.

Sample size calculation was approved by the Medical Biostatistics Unit, Faculty of Dentistry, Cairo University on 24/7/2021.

Radiographic dataset

CBCT data of this study was obtained from the CBCT data base available at the department of Oral and Maxillofacial Radiology, Faculty of Dentistry, Cairo University, Cairo, Egypt. 184 scans were obtained as a



part of the diagnosis and treatment planning for the included patients seeking extraction of their wisdom teeth.

CBCT Scans showing Mandibular third molar of patients aging from 25 to 65 years old are included in this study. The FOV used in the scans should clearly show the third molar completely with its roots and the IAN with voxel size of 0.2mm. Mandibular third molars appeared in the scans should show absence of artifacts or dental implants in the adjacent teeth.

CBCT images of sub-optimal quality or artifacts/high scatter interfering with proper assessment were excluded from the study. The imaging technique was standardized and used for all used scans. The following parameters were used: exposure time 12 seconds, voxel size 0.1-0.2 mm, field of view 5x5 - 5x8 cm, and Planmeca Promax 3D MID CBCT Machine. The study comprised 184 scans divided as the following: (59) M3M with cancellous bone separation between their roots and cortical wall of MC, (60) M3M with no cancellous bone separation between their roots and cortical wall of the MC with intact cortical wall, and (65) M3M with direct contact between their roots and cortical wall of the MC with interrupted cortical wall.

Patient declaration of consent:

Patient declaration of consent was obtained in a Helsinki declaration consent form in their native language (Arabic).

Radiographic Annotation (Ground truth)

CBCT scans were imported into the 3D Slicer software program (open-source free software version 5.2.2, Harvard University, USA) for data annotation.

The Radiologist- dependent M3M – MC relation was performed on the axial cuts and then classified into :

Class 0: Cancellous separation

Class 1: Contact with intact cortex

Class 2: contact with interrupted cortex

by 2 Oral and Maxillofacial Radiologists (OMFR) (8 & 15 years experience). This classification serves as the ground truth.

Then, the volume of interest was cropped where the apices of mandibular molar and mandibular canal are shown (Figure 2). Then, cropped scans were saved in NiTi Format from Data Module and shared with the AI team in 3 separate folders (Cancellous separation – Contact with intact cortex – contact with interrupted cortex) (Figure 2).

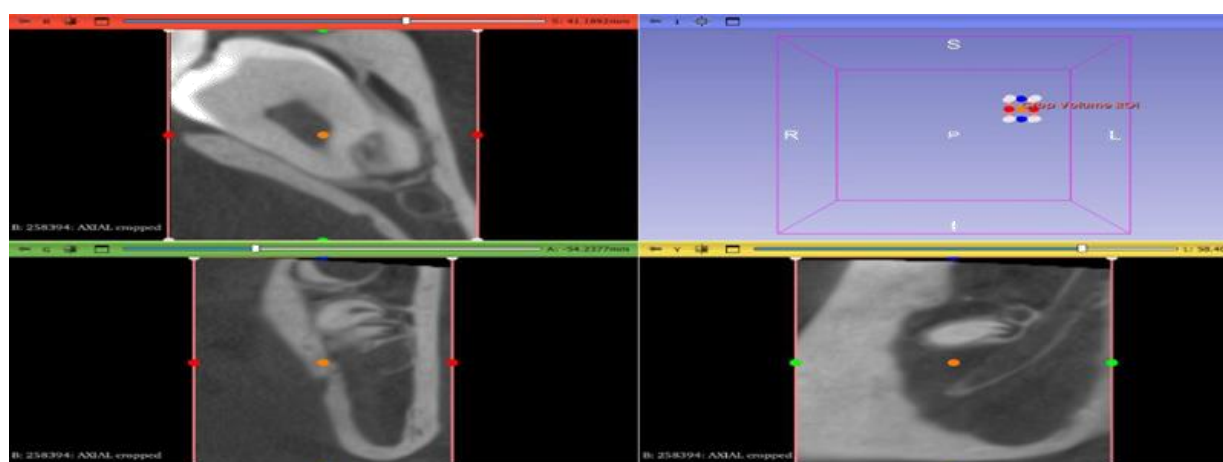


FIGURE 1– Cropped CBCT image of the roots of M3M in the axial, coronal, and sagittal direction.

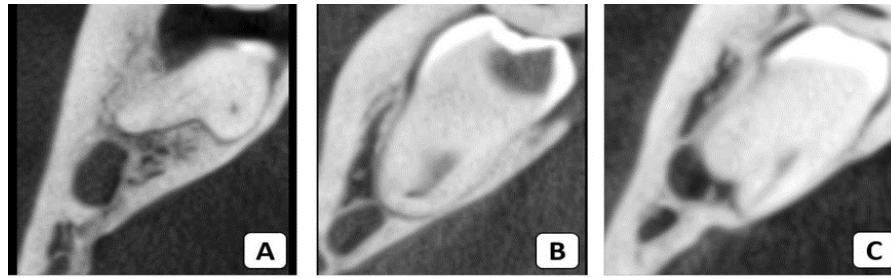


FIGURE 2– (c) Axial cuts of Cropped CBCT images representing the 3 classifications of the relation between IAC and M3M A. Cancellous bone separation, B. cortical bone separation, C. direct contact.

Development of the AI models

The classification and segmentation algorithms were developed in the Python environment (v3.9.19; Python Software Foundation, Wilmington, DE, USA) using the TensorFlow library. Mathematical processing in the model's training was performed with a Lenovo Legion y540, intel i7-9750H, 16GB DDR4 RAM, GTX 1660 ti 6GB (Lenovo Group Limited China) at the Faculty of Computer Science MSA University, Cairo, Egypt.

A total of 184 anonymized CBCT volumes with DICOM files were converted to NIFTI file format. The dataset was separated into 156 scans for training and validation and 28 scan for testing randomly. Our work approached the evaluation of the relationship between M3M and MC on CBCT images through classifying this relation into 3 classes : Class 0: Cancellous and cortical bone separation ,Class 1: Contact with intact cortex and Class 2: contact with interrupted cortex.

Therefore, the data used for training and testing was divided as the following:

Class 0: 46 scans for training and 13 for testing

Class 1: 51 scans for training and 9 for testing

Class 2: 59 scans for training and 6 for testing

The classification model uses Convolutional Neural Networks (CNNs) due to their ability to learn spatial hierarchies of features through convolutional layers. CNNs capture complex patterns like edges, textures, and shapes directly from raw images, improving computational efficiency and minimizing overfitting. They are robust to transformations like scaling, shifting,

and rotation, making them ideal for building scalable image classification models.

CNN Model architecture:

The model commenced by importing the 184 Nii pictures as sequential pngs, thereafter sampling each scan into 29 channels to extract the most pertinent slices of the volumetric data, concentrating on areas that hold substantial diagnostic significance. The sampling approach aimed to simplify the 3D Nii pictures while maintaining sufficient depth for the model to accurately differentiate between various features within the slices. The channels were regarded as distinct input layers, enabling the CNN to analyze the images as a series of interconnected 2D slices that together depict the 3D structure. Subsequently, the photos were enlarged to 224 x 224 to

standardize their dimensions, thereby easing batch processing and enhancing computational performance during training. This method guaranteed that the input data maintained a uniform size while preserving essential image properties required for precise classification, hence ensuring consistent input dimensions for the CNN model. This downsizing process also decreases the computing burden while preserving critical features required for categorization. Subsequent to scaling, each image underwent normalization to equalize pixel values, hence enhancing convergence during training by mitigating the danger of vanishing or exploding gradients. The 29 channels of each scan, denoting several slices or layers, were aggregated and regarded as separate inputs to encapsulate the depth and context of the 3D structure inherent in the original Nii pictures. These channels enabled the model to discern spatial relationships across



many levels, hence augmenting its capacity to detect nuanced patterns. This pipeline enhanced the model's performance by reconciling computational economy with the retention of essential spatial and visual information in the medical images (**Figure 3**).

The training dataset was used to train the DL model, and the validation dataset was used for early stopping criteria.

The classification model underwent training for 426 epochs with learning rate of 0.00001, the patch size was 32 and the optimizer used was Adam with a total of 1,261,979 parameter extracted. After that, the customized deep-learning model was tested on an independent test dataset, and the best model was recorded (**Figure 4**).

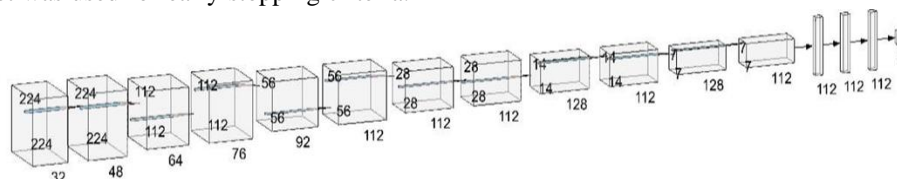


Figure 3– pipeline for the first CNN model architecture

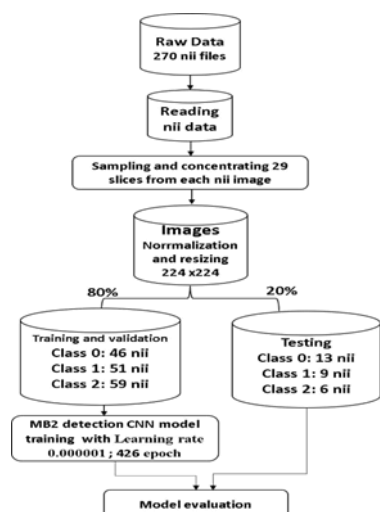


Figure 4– Diagram of the classification CNN model development steps.

Evaluation metrics:

The precision of the deep learning models (DLM) in relation to the Ground Truth (GT) was assessed using a trichotomous outcome of "presence of cancellous bone separation", "presence of cortical bone separation", and "direct contact" for each MC-M3M relation of the DLM, which was established and approved by two maxillofacial radiologists with 8 and 15 years of expertise, respectively.

The outcomes of the test group were organized into a confusion matrix comprising true positives (TP), false positives (FP), and false negatives (FN). Here, TP denotes the accurate identification of the correct class, FP signifies the erroneous identification of images containing.

Utilizing this confusion matrix, precision, recall (sensitivity), and F1 score were computed and evaluated according to the diagnostic test rankings established by Leonardi Dutra et al. [16] with corresponding scores. 80% is deemed exceptional, 70% to 80% is classified as good, 60% to 69% is seen as average, and below 60% is considered poor. The definitions of the evaluation measures are further upon in a prior work [17].

Accuracy assesses the overall correctness of the model's predictions, whereas precision and recall concentrate on the quality of positive and negative predictions, respectively. The F1 Score offers an appropriate equilibrium between precision and recall, rendering it a more equitable tool for assessing classification algorithms. The area under the curve (AUC) of the receiver operating characteristic (ROC) curve was calculated.

Results:

The simple classifier model successfully predicted the relation between the IAN and M3M through the following results :

The Average accuracy, precision, recall and F1 score for testing was 0.79, 0.77, 0.77 and 0.77 respectively, while for training was 0.9, 0.91, 0.9 and 0.9 respectively.

The results of training were shown in (**Table 1**) and the results of testing were shown in

(**Table 2**). Type II had the lowest diagnostic precision, recall and F1 score (0.67), while type 0 and 1 have comparable results.



. Confusion matrix of the results of 3 classes during training and testing presented in **Figure. 5 (a-b)**, while The Receiver-operating characteristic (ROC) curve of the 3 classes presented in **Figure. 6 (a-b-c)**.

Table 1– Results Of Training in Class 0 , 1 and 2

Train Classification Report				
	precision	recall	f1-score	support
0	0.91	0.85	0.88	46
1	0.92	0.90	0.91	51
2	0.89	0.95	0.92	59
accuracy			0.90	156
macro avg	0.91	0.90	0.90	156
weighted avg	0.90	0.90	0.90	156

Table 2– Results Of Testing in Class 0 , 1 and 2

Testing Classification Report				
	precision	recall	f1-score	support
0	0.83	0.77	0.80	13
1	0.80	0.89	0.84	9
2	0.67	0.67	0.67	6
accuracy			0.79	28
macro avg	0.77	0.77	0.77	28
weighted avg	0.79	0.79	0.78	28

Table 3– Overall Accuracy, loss and area under the curve of training and testing data

<i>c</i>	Training	Testing
<i>Accuracy</i>	0.9038	0.7857
<i>Loss</i>	0.3762	0.6397
<i>AUC</i>	0.8	0.57

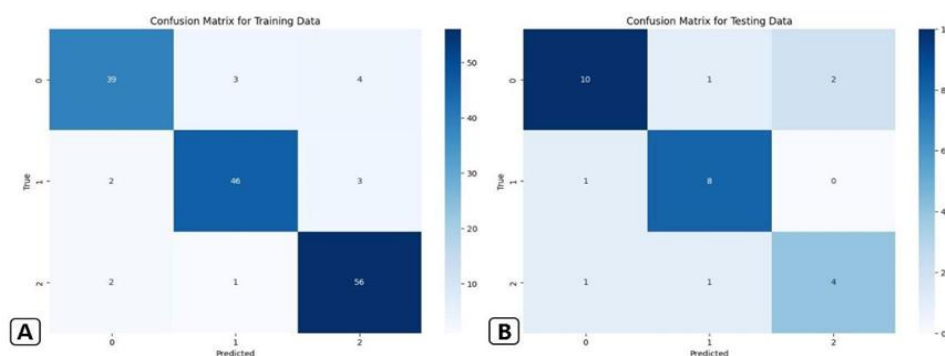


Figure 5– Confusion matrix of class 0 and 1 and 2 in A. Training Data , B. Testing Data.

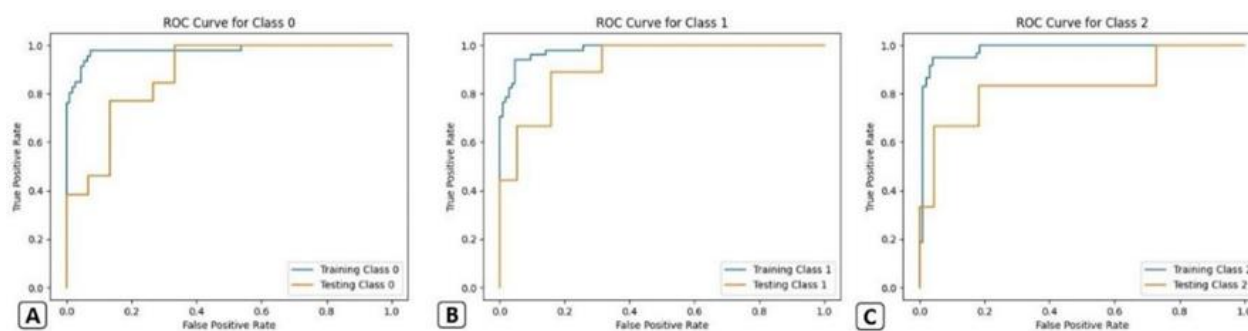


Figure 6–: Receiver-operating characteristic (ROC) curve for training and testing of A. Class 0, B. Class 1, C. Class 2.



Discussion:

The IAC injury during M3M extraction is a significant consequence and a common apprehension for both dentists and patients.[18] Despite the widespread use of panoramic radiographs to assess potential contact between M3M roots and the IAC, their prediction accuracy and reliability are significantly constrained.[19] CBCT scans have been progressively utilized for risk evaluation prior to M3M extraction. In several cases, the M3M-MC relationship observed in CBCT pictures was less distinct than that seen in apical films or panoramic radiographs, attributable to the superimposition of images on two-dimensional films.[15]

Deep learning has garnered significant attention and rapid advancement in dental imaging. [20] Numerous research have documented the utilization of CNN in assessing M3M, demonstrating encouraging outcomes in tooth growth staging [21], forecasting M3M eruption

[22], and identifying and diagnosing M3M. [12, 14] Numerous recent research have demonstrated that AI exhibits good outcomes utilizing various CNN models for the detection of M3M roots and MC contact, predominantly conducted on panoramic radiographs. (all the following)

Vranckx et al. developed a method utilizing a fully convolutional neural network with a ResNet-101 backbone to predict M3M eruption by precisely measuring molar angulations on panoramic radiographs. [22] Fukuda et al. similarly evaluated the efficacy of three CNNs in classifying the M3M-MC relationship using panoramic radiographs, reporting the highest AUC values between 0.88 and 0.93. [12, 14] Yoo et al. suggested a deep learning algorithm utilizing ResNet-34 to assess the complexity of M3M extraction operation on panoramic radiographs, employing the Pederson difficulty score.[23] This model attained precise predictions for the depth and angulation of M3M and the MC connection, with accuracy rates of 79%, 90%, and 82%, respectively. Arijj et al. utilized a U-net-based methodology to delineate and segment MC, facilitating the visualization of MC on PR and forecasting the vicinity of M3M/MC. [24] Moreover, Choi et al. revealed that a ResNet-50-based model

surpassed oral and maxillofacial surgeons in assessing the spatial relationship between M3M and MC, highlighting the inadequacy of human evaluation.[25]

Nonetheless, there is a continuous debate regarding the efficacy of CBCT in mitigating postoperative inferior alveolar nerve damage. [26] Matzen and Berkhou's meta-analysis revealed

no decrease in the incidence of IAN injuries with CBCT; nevertheless, other research indicates that CBCT may assist in predicting IAN injury occurrences and modifying treatment strategies for high-risk patients. [27] CBCT clarifies the anatomical features of M3M and MC, enhancing practitioners' confidence, particularly for those with minimal clinical expertise.[28]

In this research, we suggested and verified a one-stage CNN-based methodology, attaining great accuracy in the detection of M3M and MC, as well as in identifying their proximity utilizing CBCT images. In contrast to conventional techniques that depend on manual delineation or two-stage CNN processes, our solution employed an innovative deep learning model that necessitated solely the original image as input, thereby evading complex detection procedures and minimizing time spent. This yielded a diagnostic performance that is comparable to or exceeds that of previously described models.

Our proposed Customized CNN model exhibited commendable diagnostic performance, achieving an accuracy of 79 %, closely aligning with the assessments of residents in oral and maxillofacial radiology.

Our results surpass Orhan et al. deep CNN-based AI application that exhibits superior performance in identifying M3M and assessing the number of roots and their association with neighboring anatomical structures in CBCT, demonstrating substantial concordance with manual detection 76%. [12, 14] Nevertheless, the specifics regarding the classification of the M3M-MC relationship were not expounded upon

However, it is less than that acquired by Liu et al. utilizing ResNet-34 with overall accuracy of 93.3%.[15] This could be justified by the use of segmentation step



before the classification process performed their model which significantly improved their accuracy.

The diagnostic efficacy of M3M-MC Cnet improved due to its extensive training dataset, an altered algorithmic approach, and robust ground truth derived from CBCT, which was both objective and dependable. The uneven distribution of instances may have stemmed from the individuals who received CBCT examinations at our institution.

The use of cropped images (224 × 224 pixels) for training to minimize labor, and this dimension was adequate for accurately evaluating the relationship between the canal and molar. Moreover, the classification process of our methodology was exceptionally efficient, necessitating about 1/56 of a second per test case.

Therefore, Our technique offers enhanced convenience, reliability, efficiency, and reduced labor, as demonstrated by decreased time investment and improved predictive performance across several cohorts.

The current study has many limitations. Initially, CBCT and patient datasets were chosen from our Faculty only. Additional participants with sufficient datasets are required to enhance the generalizability and therapeutic applicability of our approach. Furthermore, the distribution of morphology and properties of M3M, including impaction depth, angulation, and root numbers, were excluded from model training. CBCT is an unequivocally reliable diagnostic tool for dental assessments and is commonly employed prior to complex tooth extractions. Our research sought to create a diagnostic instrument that assists less experienced dentists in CBCT interpretation, enabling more informed decisions regarding wisdom tooth extraction with reduced time and effort.

In conclusion, our study proposed automated diagnosis of the M3M-MC relationship by deep learning CNN model that facilitates preoperative risk evaluation and surgical strategizing, thereby minimizing postoperative inferior alveolar nerve injury. It enhances doctor-patient communication by offering clear visualizations and dependable evaluations which revolutionize clinical

practices by delivering swift, precise, and effective diagnostic instruments for assessing the correlation between M3M and MC. These advances are expected to improve patient outcomes and optimize surgical workflows.

References:

- [1] G. D and G. KL, "Sensory impairment of the lingual and inferior alveolar nerves following removal of impacted mandibular third molars - PubMed," *International journal of oral and maxillofacial surgery*, vol. 30, no. 4, 2001 Aug, doi: 10.1054/ijom.2001.0057.
- [2] G. H, M. GJ, S. A, B. WA, M. J, and B. SJ, "Position of the impacted third molar in relation to the mandibular canal. Diagnostic accuracy of cone beam computed tomography compared with panoramic radiography - PubMed," *International journal of oral and maxillofacial surgery*, vol. 38, no. 9, 2009 Sep, doi: 10.1016/j.ijom.2009.06.007.
- [3] A. B. Tay and W. S. Go, "Effect of exposed inferior alveolar neurovascular bundle during surgical removal of impacted lower third molars," (in eng), *J Oral Maxillofac Surg*, vol. 62, no. 5, pp. 592-600, May 2004, doi: 10.1016/j.joms.2003.08.033.
- [4] W. Tantanapornkul *et al.*, "A comparative study of cone-beam computed tomography and conventional panoramic radiography in assessing the topographic relationship between the mandibular canal and impacted third molars," *Oral Surgery, Oral Medicine, Oral Pathology, Oral Radiology and Endodontics*, vol. 103, no. 2, 2007/02/01, doi: 10.1016/j.tripleo.2006.06.060.
- [5] W. D. Vos, J. Casselman, and G. R. J. Swennen, "Cone-beam computerized tomography (CBCT) imaging of the oral and maxillofacial region: A systematic review of the literature," *International Journal of Oral and Maxillofacial Surgery*, vol. 38, no. 6, 2009/06/01, doi: 10.1016/j.ijom.2009.02.028.
- [6] P. PS, S. JS, D. BB, B. PB, J. YV, and M. RS, "Comparison of panoramic radiograph and cone beam computed tomography findings for impacted



- mandibular third molar root and inferior alveolar nerve canal relation - PubMed," *Indian journal of dental research : official publication of Indian Society for Dental Research*, vol. 31, no. 1, 2020 Jan-Feb, doi: 10.4103/ijdr.IJDR_540_18.
- [7] H. Ghaemina *et al.*, "The use of cone beam CT for the removal of wisdom teeth changes the surgical approach compared with panoramic radiography: a pilot study," *International Journal of Oral and Maxillofacial Surgery*, vol. 40, no. 8, 2011/08/01, doi: 10.1016/j.ijom.2011.02.032.
- [8] V. Gulshan *et al.*, "Accuracy of a Deep Learning Algorithm for Detection of Diabetic Retinopathy," *JAMA*, vol. 316, no. 22, 2016/12/13, doi: 10.1001/jama.2016.17216.
- [9] A. Esteva *et al.*, "Dermatologist-level classification of skin cancer with deep neural networks," *Nature* 2017 542:7639, vol. 542, no. 7639, 2017-01-25, doi: 10.1038/nature21056.
- [10] T. Hiraiwa *et al.*, "A deep-learning artificial intelligence system for assessment of root morphology of the mandibular first molar on panoramic radiography," *Dentomaxillofacial Radiology*, vol. 48, no. 3, 2019/03, doi: 10.1259/dmfr.20180218.
- [11] G. H. Kwak *et al.*, "Automatic mandibular canal detection using a deep convolutional neural network," *Scientific Reports*, vol. 10, no. 1, 2020, doi: 10.1038/s41598-020-62586-8.
- [12] M. Fukuda *et al.*, "Comparison of 3 deep learning neural networks for classifying the relationship between the mandibular third molar and the mandibular canal on panoramic radiographs," *Oral Surgery, Oral Medicine, Oral Pathology and Oral Radiology*, vol. 130, no. 3, 2020/09/01, doi: 10.1016/j.oooo.2020.04.005.
- [13] J.-H. Yoo *et al.*, "Deep learning based prediction of extraction difficulty for mandibular third molars," *Scientific Reports*, vol. 11, no. 1, 2021, doi: 10.1038/s41598-021-81449-4.
- [14] K. Orhan, E. Bilgir, I. S. Bayrakdar, M. Ezhov, M. Gusarev, and E. Shumilov, "Evaluation of artificial intelligence for detecting impacted third molars on cone-beam computed tomography scans," *Journal of Stomatology, Oral and Maxillofacial Surgery*, vol. 122, no. 4, 2021/09/01, doi: 10.1016/j.jormas.2020.12.006.
- [15] L. MQ *et al.*, "Deep learning-based evaluation of the relationship between mandibular third molar and mandibular canal on CBCT - PubMed," *Clinical oral investigations*, vol. 26, no. 1, 2022 Jan, doi: 10.1007/s00784-021-04082-5.
- [16] L. D. K *et al.*, "Diagnostic Accuracy of Cone-beam Computed Tomography and Conventional Radiography on Apical Periodontitis: A Systematic Review and Meta-analysis - PubMed," *Journal of endodontics*, vol. 42, no. 3, 2016 Mar, doi: 10.1016/j.joen.2015.12.015.
- [17] Ş. B. Duman *et al.*, "Second mesiobuccal canal segmentation with YOLOv5 architecture using cone beam computed tomography images," *Odontology*, vol. 112, no. 2, pp. 552-561, 2024.
- [18] K. Carter, S. Worthington, and S. W. K. Carter, "Predictors of Third Molar Impaction," *Journal of Dental Research*, vol. 95, no. 3, 2015-11-11, doi: 10.1177/0022034515615857.
- [19] L. K. Cheung, Y. Y. Leung, L. K. Chow, M. C. M. Wong, E. K. K. Chan, and Y. H. Fok, "Incidence of neurosensory deficits and recovery after lower third molar surgery: a prospective clinical study of 4338 cases," *International Journal of Oral and Maxillofacial Surgery*, vol. 39, no. 4, 2010/04/01, doi: 10.1016/j.ijom.2009.11.010
- [20] H. T *et al.*, "A deep-learning artificial intelligence system for assessment of root morphology of the mandibular first molar on panoramic radiography - PubMed," *Dento maxillo facial radiology*, vol. 48, no. 3, 2019 Mar, doi: 10.1259/dmfr.20180218.
- [21] N. Banar *et al.*, "Towards fully automated third molar development staging in panoramic radiographs," *International Journal of Legal*



- Medicine* 2020 134:5, vol. 134, no. 5, 2020-04-01, doi: 10.1007/s00414-020-02283-3.
- [22] M. Vranckx *et al.*, "Artificial Intelligence (AI)-Driven Molar Angulation Measurements to Predict Third Molar Eruption on Panoramic Radiographs," *International Journal of Environmental Research and Public Health*, vol. 17, no. 10, 2020/05, doi:10.3390/ijerph17103716.
- [23] J.-H. Yoo *et al.*, "Deep learning based prediction of extraction difficulty for mandibular third molars," *Scientific Reports* 2021 11:1, vol. 11, no. 1, 2021-01-21, doi: 10.1038/s41598-021-81449-4.
- [24] Y. Arijji, M. Mori, M. Fukuda, A. Katsumata, and E. Arijji, "Automatic visualization of the mandibular canal in relation to an impacted mandibular third molar on panoramic radiographs using deep learning segmentation and transfer learning techniques," *Oral Surgery, Oral Medicine, Oral Pathology and Oral Radiology*, vol. 134, no. 6, 2022/12/01, doi:10.1016/j.oooo.2022.05.014.
- [25] E. Choi *et al.*, "Artificial intelligence in positioning between mandibular third molar and inferior alveolar nerve on panoramic radiography," *Scientific Reports* 2022 12:1, vol. 12, no. 1, 2022-02-14, doi: 10.1038/s41598-022-06483-2.
- [26] W. Qi, J. Lei, Y.-N. Liu, J.-N. Li, J. Pan, and G.-Y. Yu, "Evaluating the risk of post-extraction inferior alveolar nerve injury through the relative position of the lower third molar root and inferior alveolar canal," *International Journal of Oral and Maxillofacial Surgery*, vol. 48, no. 12, 2019/12/01, doi: 10.1016/j.ijom.2019.07.008.
- [27] M. LH and B. E, "Cone beam CT imaging of the mandibular third molar: a position paper prepared by the European Academy of DentoMaxilloFacial Radiology (EADMFR) - PubMed," *Dento maxillofacial radiology*, vol. 48, no. 5, 2019 Jul, doi: 10.1259/dmfr.20190039.
- [28] J. Szalma, L. Vajta, B. V. Lovász, C. Kiss, B. Soós, and E. Lempel, "Identification of Specific Panoramic High-Risk Signs in Impacted Third Molar Cases in Which Cone Beam Computed Tomography Changes the Treatment Decision," *Journal of Oral and Maxillofacial Surgery*, vol. 78, no. 7, 2020/07/01, doi: 10.1016/j.joms.2020.03.012.